




Intratumoral co-injection of the poly I:C-derivative BO-112 and a STING agonist synergize to achieve local and distant anti-tumor efficacy

Maite Alvarez ,^{1,2,3} Carmen Molina,^{1,2} Carlos E De Andrea,^{2,3,4} Myriam Fernandez-Sendin,^{1,2} Maria Villalba,^{3,4} Jose Gonzalez-Gomariz,¹ Maria Carmen Ochoa,^{1,2,3} Alvaro Teijeira,^{1,2,3} Javier Glez-Vaz,^{1,2} Fernando Aranda,^{1,2} Miguel F Sanmamed,^{1,2,3,5} Maria E Rodriguez-Ruiz,⁵ Xinyi Fan,⁶ Wen H Shen,⁶ Pedro Berraondo ,^{1,2,3} Marisol Quintero,⁷ Ignacio Melero ^{1,2,3,5}

To cite: Alvarez M, Molina C, De Andrea CE, *et al.* Intratumoral co-injection of the poly I:C-derivative BO-112 and a STING agonist synergize to achieve local and distant anti-tumor efficacy. *Journal for ImmunoTherapy of Cancer* 2021;**9**:e002953. doi:10.1136/jitc-2021-002953

► Additional supplemental material is published online only. To view, please visit the journal online (<http://dx.doi.org/10.1136/jitc-2021-002953>).

Accepted 28 September 2021



© Author(s) (or their employer(s)) 2021. Re-use permitted under CC BY-NC. No commercial re-use. See rights and permissions. Published by BMJ.

For numbered affiliations see end of article.

Correspondence to

Dr Ignacio Melero;
imelero@unav.es

Dr Maite Alvarez;
malvarezr@unav.es

ABSTRACT

Background BO-112 is a nanoplexed form of polyinosinic:polycytidylic acid that acting on toll-like receptor 3 (TLR3), melanoma differentiation-associated protein 5 (MDA5) and protein kinase RNA-activated (PKR) elicits rejection of directly injected transplanted tumors, but has only modest efficacy against distant untreated tumors. Its clinical activity has also been documented in early phase clinical trials. The 5,6-dimethylxanthenone-4-acetic acid (DMXAA) stimulator of interferon genes (STING) agonist shows a comparable pattern of efficacy when used via intratumoral injections.

Methods Mice subcutaneously engrafted with bilateral MC38 and B16.OVA-derived tumors were treated with proinflammatory immunotherapy agents known to be active when intratumorally delivered. The combination of BO-112 and DMXAA was chosen given its excellent efficacy and the requirements for antitumor effects were studied on selective depletion of immune cell types and in gene-modified mouse strains lacking basic leucine zipper ATF-like transcription factor 3 (BATF3), interferon- α/β receptor (IFNAR) or STING. Spatial requirements for the injections were studied in mice bearing three tumor lesions.

Results BO-112 and DMXAA when co-injected in one of the lesions of mice bearing concomitant bilateral tumors frequently achieved complete local and distant antitumor efficacy. Synergistic effects were contingent on CD8 T cell lymphocytes and dependent on conventional type 1 dendritic cells, responsiveness to type I interferon (IFN) and STING function in the tumor-bearing host. Efficacy was preserved even if BO-112 and DMXAA were injected in separate lesions in a manner able to control another untreated third-party tumor. Efficacy could be further enhanced on concurrent PD-1 blockade.

Conclusion Clinically feasible co-injections of BO-112 and a STING agonist attain synergistic efficacy able to eradicate distant untreated tumor lesions.

INTRODUCTION

Intratumoral delivery of immunotherapy agents offers some advantages in terms of

safety and localized pharmacodynamics.^{1,2} A number of agents have been intratumorally tested in mouse models with the intention to create ‘in situ’ cancer vaccines³ that would be able to control untreated metastasis or micrometastasis in the tumor-bearing host as a result of enhanced antitumor immunity. Virotherapy armed or not with immune transgenes,⁴ microbial molecular pattern receptor agonists,⁵ recombinant proteins,² antibodies,⁶ mRNA⁷ and even adoptive immunotherapy⁸ have shown efficacy in animal models. Such strategies are feasible in the clinic and promising results have been reported, especially on intratumoral delivery of herpes virus vectors,⁹ unmethylated cytosine-phosphate-guanine (CpG) oligonucleotides^{10,11} and viral RNA mimetics based on polyinosinic:polycytidylic acid (poly I:C),^{12,13} mRNAs¹⁴ and cDNA plasmids.¹⁵ Lesions located in the skin or close to the body surface are preferred, but image-guided injections are feasible and convenient.¹⁶

BO-112 is a poly I:C moiety that is nanoparticled on conjugation to polyethylenimine.^{17,18} Its effects on toll-like receptor (TLR)3, melanoma differentiation-associated protein 5 (MDA5) and protein kinase RNA-activated (PKR) explain the observed potent activities on innate immune signaling, acting as a RNA-viral mimetic.^{17–19} Experiments in mouse-transplanted models¹⁷ showed that intratumoral injection of BO-112 was able to elicit potent local antitumor effects that were contingent on the immunocompetence of the mice treated. Immunogenic cell death and cross-priming of tumor antigens are involved, as well as activation signals in antigen-presenting cells in an environment enriched

with type I interferons. Mice rejecting tumors became immune to rechallenge, but efficacy against distantly implanted untreated tumor lesions was seldom observed. Combinations with costimulatory anti-programmed cell death protein 1 (PD-1) and anti-CD137 monoclonal antibodies enhanced such therapeutic effects at least to some extent. Given the preclinical efficacy and safety profile of this drug, clinical trials are in progress (NCT04525859, NCT04420975, NCT04508140) following published clinical evidence for safety and activity on combination with pembrolizumab and nivolumab in a few checkpoint-inhibitor refractory patients.¹²

The cyclic GMP-AMP synthase (cGAS)/stimulator of interferon genes (STING) pathway is also critical for induction of innate immunity to pathogens and tumors.²⁰ In mice, the STING agonist 5,6-dimethylxanthenone-4-acetic acid (DMXAA) on intratumoral delivery has been shown to cause tumor regression also mediated by innate and adaptive immune responses.^{21,22} Bilateral efficacy against untreated concomitant tumors was reported in some instances.²¹ DMXAA, which is readily active on mouse STING, is not active on most allelic variants of human STING,²¹ even though other synthetic STING agonists have been developed and tested in clinical trials with thus far weak signals of therapeutic activity following local therapy, either as single agents or combined with systemic anti-PD-1 monoclonal antibodies.^{23,24}

Given the fact that BO-112 and DMXAA act on different, but partially overlapping pathways, we tested the combination of such agents for intratumoral injections and discovered powerful synergistic activities able to control untreated distant disease.

MATERIAL AND METHODS

Mice

C57BL/6 and BALB/c mice were purchased from Harlan Laboratories (Barcelona, Spain). C57BL/6 Batf3tm1K-mm/J (basic leucine zipper ATF-like transcription factor 3 (BATF3) knockout (KO))²⁵ or wild type (WT) counterparts were kindly provided by Dr Kenneth M Murphy (Washington University, St. Louis, Missouri, USA) and bred at the Center for Applied Medical Research (CIMA) animal facility. C57BL/6 interferon (IFN)- α /bR^{o/o} (IFNAR KO)²⁶ and C57BL/6 Tmem173^{fl}/J (STING KO)²⁷ were kindly gifted by Dr Matthew Albert (Institut Pasteur, Paris) and Dr Gloria Gonzalez Aseguinolaza (CIMA, Spain), respectively, and bred at the CIMA animal facility. Female mice were used at 8–12 weeks of age and housed under specific pathogen-free conditions.

Cell lines and cell cultures

B16-OVA mouse melanoma cells and MC38 mouse colon carcinoma cell lines were kindly gifted by Dr Lieping Chen (Yale University, New Haven, Connecticut, USA) and Dr Karl E Hellström (University of Washington, Seattle, Washington, USA), respectively. Cells were grown in Roswell Park Memorial Institute 1640 media supplemented with

GlutaMAX (Gibco), 10% heat-inactivated fetal bovine serum (FBS), 50 μ M 2-mercaptoethanol, 100 U/mL penicillin, and 100 μ g/mL streptomycin at 37°C with 5% CO₂ (complete media). B16.OVA tumor cells were grown in complete media supplemented with 400 μ g/mL Geneticin (Gibco). Cells were collected for tumor studies when they reached exponential growth during that week of culture. The CD8 α ⁺ conventional type 1 dendritic cells (cDC1)-like MutuDC1 cell line was kindly provided by Dr Hans Acha-Orbea (University of Lausanne, Epalinges, Switzerland) and grown as previously described.²⁸ Bone marrow-derived cDC1 were generated from C57BL/6 mice as previously described.²⁹ All cell lines were tested monthly for mycoplasma contamination (MycoAlert Mycoplasma Detection Kit, Lonza).

Mouse tumor models

To determine the abscopal effect, and depending on the mouse tumor model, 4 \times 10⁵ MC38, B16.OVA or mouse mammary adenocarcinoma TSA tumor cells were subcutaneously injected into the right flank of C57BL/6 (MC38 or B16.OVA) or BALB/c (TSA) mice, whereas the left flank received a subcutaneous injection of 2 \times 10⁵ (MC38 or TSA) or 1.25 \times 10⁵ (B16.OVA) tumor cells. When right tumors reached a tumor volume of 40–50 mm³ (approximately 1 week after tumor inoculation), mice were randomized into different treatment groups and, depending on the experiment, right tumors were injected intratumorally with 50 μ g of BO-112 (Highlight Therapeutics, Valencia, Spain) and/or 100 μ g of STING ligand DMXAA (Invivogen, Toulouse France), 50 μ g of TLR9 ligand CpG oligodeoxynucleotides (ODN) 1585 (Invivogen), CpG ODN 1668 (Invivogen), CpG ODN 2395 (Invivogen), or 30 μ g agonistic anti-CD40 (BioXcell, Lebanon, NH). Control mice received intratumoral injections of phosphate buffered saline (PBS) containing 5% glucose and/or 5% dimethyl sulfoxide (DMSO), negative ODN control (Invivogen) or rIgG (BioXcell) when appropriate. Treated and untreated tumors were measured twice a week with calipers and the volume was calculated (length \times width²/2). Additionally, mice were monitored for survival and euthanized when any tumor size reached a diameter of 15 mm or mice displayed signs of distress. In some experiments, C57BL/6 mice deficient for BAFT3, interferon α / β receptor (IFNAR)1 or STING or their WT counterparts were used.

For selective depletion studies of immune cell subsets, mice were intraperitoneally treated with 100 μ g, anti-NK1.1 (clone PK136, BioXcell), anti-CD8 β (clone Lyt3.2, BioXcell) or anti-CD4 (clone GK1.5, BioXcell) on days 6 and 9 after tumor inoculation followed by weekly intraperitoneal injections until the end of the experiment to deplete NK, CD8 and CD4 T cells, respectively, without altering CD8⁺ DC. Control mice received intraperitoneal injections of rat IgG (BioXcell).

In some experiments, daily intraperitoneal injections of 50 μ g of the sphingosine 1-phosphate inhibitor FTY720 (Sigma-Aldrich) or PBS were given to some mice for the

duration of the BO-112/DMXAA regimen to evaluate the role of T cell recirculation in the MC38 bilateral tumor mouse model.

To evaluate the spatial requirements for co-injections of BO-112 and DMXAA, 4×10^5 MC38 tumor cells were injected subcutaneously into the left and right flanks, and 2×10^5 tumor cells were injected subcutaneously in the upper dorsal region. When right and left tumors reached $80\text{--}100\text{mm}^3$, mice were randomized to three groups. The control group received intratumoral injections of 5% glucose and 5% DMSO in PBS to both right and left tumors, a BO-112 +DMXAA group received BO-112 and DMXAA intratumoral injections in the right tumor, and BO-112/DMXAA group received BO-112 intratumoral injection in the right tumor, but DMXAA in the left tumor. The untreated third-party tumor was left untouched in all groups. Similar experiments were performed in the MC38 bilateral tumor model separately treating the tumors.

PD-1 blockade therapy was provided by intraperitoneal $100\mu\text{g}$ anti-PD-1 (clone RMP1-14, BioXcell) on days 8, 10 and 12. Control mice received intraperitoneal injections of rat IgG.

Flow cytometry

For analysis of the immune cell component in tumors, draining lymph nodes (dLN) and spleen, MC38 or B16.OVA tumor-bearing mice were treated with vehicle control, BO-112 and/or DMXAA when right tumors reached 80mm^3 . Organs were collected at the indicated time points following completion of treatments with two doses of BO-112 and/or DMXAA. Organs were mechanically disrupted, and single-cell suspensions were generated as previously described.¹⁷ The distribution of immune cells in tumors, tumor dLNs and spleen was evaluated by flow cytometry. Single-cell suspensions were stained with monoclonal antibody (mAb) as previously described.^{30 31} Additionally, the CD8 T cell compartment (CD45+CD19-TCR β +NK1.1-CD8+CD4-) was analyzed for antigen specificity (gp70 pentamer or MHC tetramer H-2K^b OVA SIINFEKL). The Foxp3/TF staining buffer kit (eBioscience, San Diego, California, USA) was used according to manufacturer's instructions for intracellular staining. CD4 T cells and Tregs were defined as CD45+CD19-TCR β +NK1.1-CD8-CD4+Foxp3- and CD45+CD19-TCR β +NK1.1-CD8-CD4+CD25+Foxp3+, respectively. For analysis of DC subsets, cells were gated as CD45+CD19-F4/80-TCR β -NK1.1-MHCII+CD11c+ and further identified as cDC1 (CD11b-) or cDC2 (CD11b+). Monocytes/macrophages were identified as CD45+CD19-TCR β -NK1.1-CD11b+Ly6C+. In *in vitro* experiments using cDC1 cells, the expression of CD40, CD80 and CD86 maturation markers as median fluorescence intensity were evaluated in cDC1 cells (CD45+CD11c+MHCII+CD24+CD11b-CD103+XCR1+). For a detailed description of the mAbs used see online supplemental table 1. Stained cells were analyzed with Cytoflex LX (Beckmann Coulter, Indianapolis, Indiana, USA). Fluorescence minus one or biological

comparison controls were used for cell analysis. FlowJo software (TreeStar) was used for data analysis.

Multiplexed immunofluorescence staining

A five-color multiplex immunofluorescence panel based on tyramide signal amplification was used for simultaneous detection of CD3 (T cells), CD8 (cytotoxic T lymphocytes (CTLs)), Foxp3 (regulatory T cells), Ki67 (proliferating cells) and diamidino-2-phenylindole (DAPI) on tumor sections from formalin-fixed paraffin-embedded (FFPE) samples. The validation pipeline for the multiplex immunofluorescence protocol has been previously described by our group.³² Briefly, $4\mu\text{m}$ thick sections obtained from FFPE tissue blocks were deparaffinized and rehydrated from ethanol to water. Antigen retrieval with citrate (pH6, PerkinElmer) or EDTA (pH9, Dako) target retrieval solution was performed at the beginning of each sequential round of antibody staining. Each round consisted of heat-induced antigen retrieval followed by protein blocking (Antibody Diluent/Block, Akoya Bioscience), incubation with primary antibody, anti-rabbit secondary antibody (Opal Polymer anti-rabbit horseradish peroxidase Kit, Perkin Elmer) finishing with Opal fluorophore incubation diluted in 1XPlus Amplification Diluent (Akoya Bioscience). The panel included the following primary antibodies: CD3 (rabbit monoclonal, clone SP7, 1:100, Abcam, REF. ab16669), CD8 (rabbit monoclonal, clone D4W2Z, 1:500, Cell Signaling Technology, REF. 98941), Foxp3 (rabbit monoclonal, clone D6O8R, 1:500, Cell Signaling Technology, REF. 12653) and Ki67 (rabbit polyclonal, 1:500, Abcam, REF. ab15580). At the end of the protocol, nuclei were counterstained with spectral DAPI (Akoya Biosciences) and sections were mounted with Faramount Aqueous Mounting Medium (Dako).

Whole tissue sections were scanned on a Vectra-Polaris Automated Quantitative Pathology Imaging System (Akoya Biosciences). Akoya Biosciences' Inform software (V.2.4.8) was used to remove the autofluorescence determined by an unstained slide and to perform the spectral unmixing of the images. Informative fields were selected for microphotography.

Serum cytokine analysis

The level of cytokines in the serum or supernatant of cell cultures was measured using a multiplex assay (Luminex MAGPIX Instrument System, Thermo Fisher Scientific, Waltham, Massachusetts, USA) with a custom designed Cytokine 13-Plex Mouse ProcartaPlex Panel (Thermo Fisher Scientific, Waltham, Massachusetts, USA) following the manufacturer's instructions.

Crispr/Cas9 sting knockout

TSA parental, CRISPR/Cas9 mock-silenced and STING-silenced variants were generated in Dr Wen H Shen's laboratory (Weill Cornell Medicine) and grown in Dulbecco's Modified Eagle Medium (DMEM) media supplemented with 10% FBS and $50\mu\text{M}$ 2-mercaptoethanol. TSA tumor cells were then transfected with pSpCas9(BB)-2A-Puro

(PX459) V2.0 (Addgene #62988) for 48 hours. After transfection, cells were treated with 2.0 µg/mL puromycin for 48 hours. The remaining live cells were plated to a 96-well plate. Single clones were picked up and western blot using the monoclonal antibody anti-STING clone D2P2F (Cell Signaling Technology) was performed for STING KO verification following manufacturer's instructions. Single-guide (sgRNA) sequences used to delete the Sting gene were Exon1-guide1F caccg CAGTAGTCCAAGTTCGTGCG and Exon1-guide1R aaac CGCACGAACTTGGACTACTGc.

RNA sequencing and data analysis

MC38-derived treated tumors were collected 24 hours following a single dose of vehicle control, BO-112 and/or DMXAA. Treated tumors were collected in RNeasy lysis buffer (Sigma-Aldrich) and stored at -20°C until further processing. Total RNA was isolated using RNeasy Midi isolation kit (Qiagen) according to manufacturer's instructions. RNA sequencing was prepared using the TruSeq Stranded mRNA LT Sample Prep Kit (Illumina, California, USA) under standard protocol. The quality and quantity of samples used for RNAseq analysis were examined using an RNA 6000 Nano LabChip on a 2100 Bioanalyzer (Agilent Technologies) and Qubit 2.0. Then, RNAseq was conducted on 15 samples on the Illumina NovaSeq6000 platform. Raw RNA-Seq reads were deposited in the gene expression Omnibus (GEO) database of the National Center for Biotechnology Information and are accessible through GEO Series accession number GSE184157 (<https://www.ncbi.nlm.nih.gov/geo/query/acc.cgi?acc=GSE184157>).

For RNAseq data analysis, first, quality control of all samples were performed with FastQC tool (<http://www.bioinformatics.bbsrc.ac.uk/projects/fastqc>). Before alignment, reads with low quality and adapters were removed using Trimmomatic.³³ Matrix of raw counts was obtained using STAR aligner³⁴ with mm39 assembly and annotated with Gencode V.M27. The analysis of differentially expressed genes was carried out following the bioinformatics workflow provided by limma to allow the analysis of RNAseq experiments using linear models. First, the data sets were normalized using the trimmed mean of M-values normalization, then the log₂ counts per million values were calculated using voom from limma package and the normalized expression matrix was used for statistical analysis with limma.³⁵ Genes with less than five counts in all the samples (non-expressed genes) were removed from the analysis before normalization. We selected the set of genes differentially expressed for each comparison using the criteria of *p* value <0.05.

Statistical analysis

Each experiment was performed using five to six mice per group. A one-way analysis of variance (ANOVA) test with Tukey's post-test analysis, a two-way ANOVA test with Tukey's post-test analysis, and a log-rank test were used, when appropriate, to determine statistical significance

(GraphPad Prism V.6.0, La Jolla, California, USA). *P* values were considered statistically significant when *p*<0.05.

RESULTS

Intratumoral co-injection of nanoplexed poly I:C (BO-112) and the DMXAA STING agonist synergize to control treated and untreated tumor lesions

Distant efficacy following intratumoral immunotherapy is crucial to achieve clinically meaningful results. Therefore, we comparatively tested several immunotherapy agents therapeutically active following repeated intratumoral injections, and tumor growth was followed over time both in treated and untreated tumor lesions. Groups of mice bearing bilateral MC38-derived tumors, as schematized in [figure 1A](#), were treated with the different agents and schedules. The directly injected tumors remarkably responded to the treatment with BO-112, as well as to treatments with the DMXAA STING agonist and class B and C CpG oligonucleotides, which resulted in the complete regression of 60%–100% of the tumors ([figure 1B–C](#)). In contrast, untreated contralateral tumors lethally progressed in most animals independently of the treatment, although with some observable delays in their growth and a few cases of bilateral efficacy for CpG oligonucleotides ([figure 1B–D](#)).

Next, we examined if intratumoral co-injections of two agents could attain better efficacy on the untreated lesions repressing distant metastatic disease ([figure 2](#)). As shown in [figure 2A](#), co-injections of BO-112 and the DMXAA STING agonist at the same dosages as in [figure 1A](#) in MC38 tumors were able to completely control the injected lesions and to eradicate distant disease in 6 out of 12 instances, showing clear delays in tumor growth in those animals that did not achieve complete rejection ([figure 2C](#)). Such combined efficacy was leading to long-term survival ([figure 2E](#)). Local and systemic efficacy was also substantiated against B16.OVA bilaterally engrafted tumors with 2 out of 10 mice surviving long term ([figure 2B, D and F](#)).

Intratumoral co-injections of BO-112 with other agents such as agonistic anti-CD40 mAb and class A to C CpG oligonucleotides did not achieve synergistic effects against untreated malignant lesions (online supplemental figure 1). Given these findings, we decided to focus on co-injections of BO-112 and STING agonists for local and systemic cancer treatments.

Antitumor CD8+ T cell lymphocytes underlie the intratumoral co-injection effects of BO-112 and DMXAA

The activity of both BO-112 and STING agonist agents is reportedly due to the activity of CD8 T cells.^{17 21 22} Accordingly, we decided to study if intratumoral co-injections could lead to stronger CD8 T cell-mediated antitumor effects. To that end, tumors treated as in [figure 1A](#) were surgically excised on day 11, when effects on tumor size started to be macroscopically evident ([figure 3A](#)) and cell

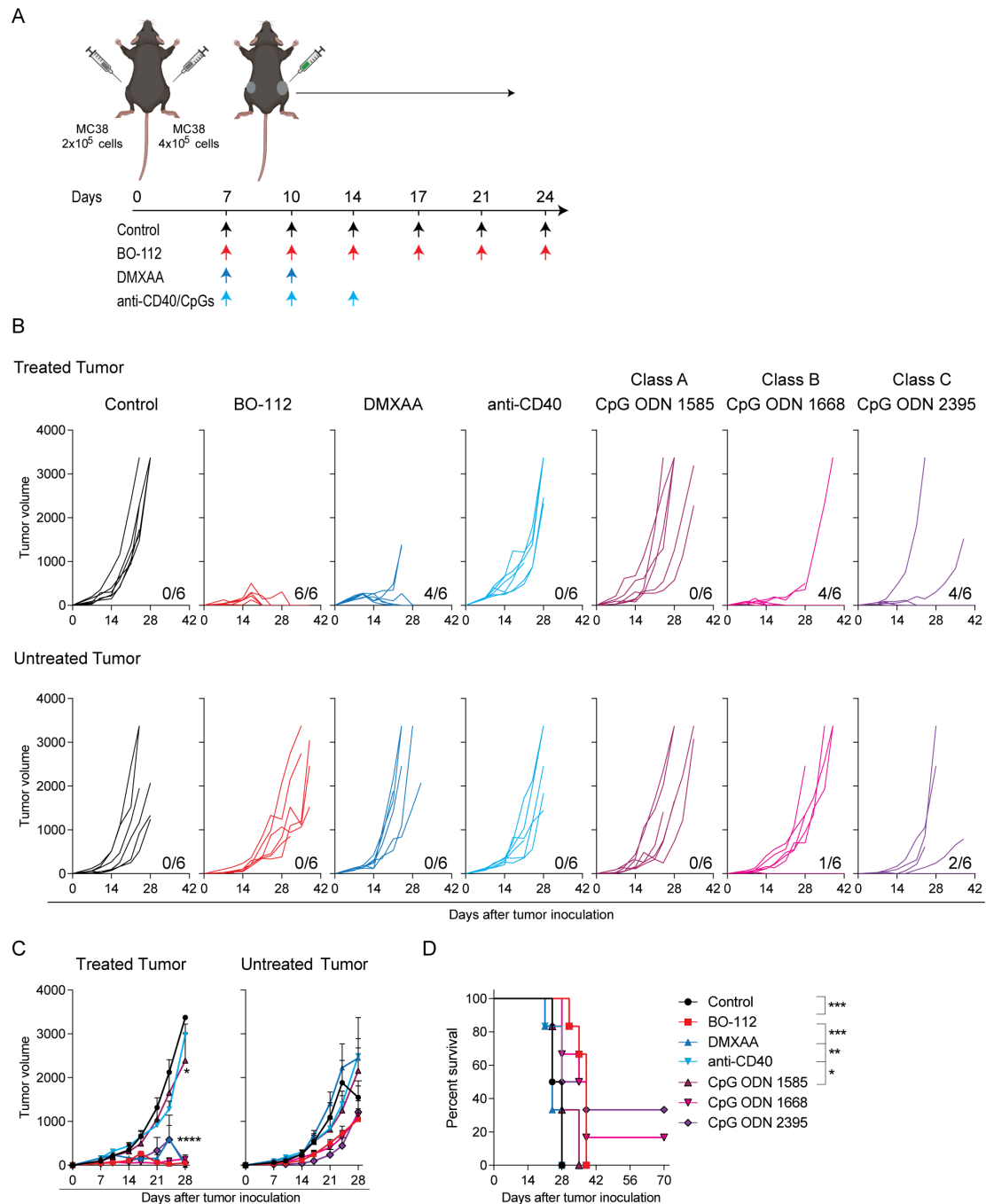


Figure 1 Intratumoral immunotherapy agents control directly injected tumor lesions but not distantly engrafted tumors. MC38 tumor-bearing C57BL/6 mice were treated intratumorally with 50 μ g of BO-112, 100 μ g of STING ligand 5,6-dimethylxanthenone-4-acetic acid (DMXAA), 30 μ g of anti-CD40, or 50 μ g of toll-like receptor 9 agonists. Rat IgG/dimethyl sulfoxide/oligodeoxynucleotides control was used in control mice. (A) Schematic representation of the dosing time course and regimen followed for each treatment. (B) The tumor growth (mm^3) is shown for each individual mouse in treated (upper panels) and untreated (lower panels) tumors. The numbers under each graph represent the fraction of mice that achieved complete tumor regression for each tumor type. (C) The average of in vivo tumor growth is shown for treated (left panel) and untreated (right panel) tumors. (D) The percentage of survival over time is shown for experiments in B. Data are representative of three independent experiments with six mice per group (mean \pm SEM). Two-way analyses of variance (ANOVAs) (C) or log-rank (D) tests were used to assess significance. Significant differences are displayed for comparisons of each group with the BO-112 group (** $p < 0.01$, *** $p < 0.001$, **** $p < 0.0001$).

suspensions from such tumors were analyzed by multiparametric flow cytometry. Intratumoral BO-112 and DMXAA-treated tumors showed synergistic evidence of containing larger quantities of CD8 T cells per gram of

tumor tissue when compared with BO-112 or DMXAA single-agent treated tumors or tumors injected with vehicle (figure 3B). Co-treatments resulted in higher CD8 to Treg ratios (figure 3C). Moreover, when analyzing CD8

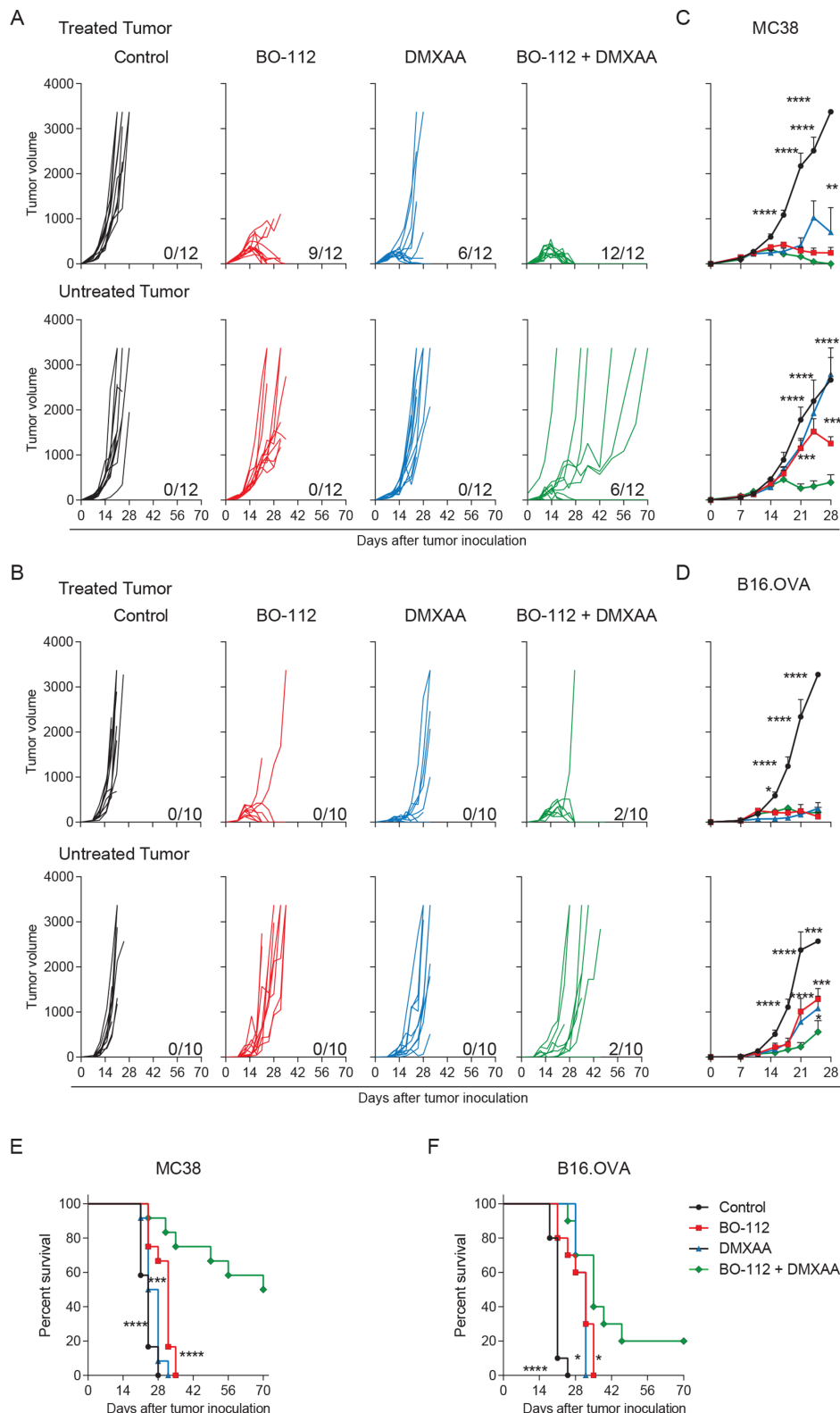


Figure 2 Synergistic local and abscopal efficacy of intratumoral co-injections of BO-112 and the DMXAA STING agonist. (A–B) The in vivo tumor growth (mm³) for individual MC38 (A) or B16.OVA (B) tumor-bearing mice is shown for treated (upper panels) and untreated (lower panels) tumors. (C–D) The means (\pm SEM) of tumor size volume (mm³) for in vivo tumor progression are shown for treated (upper panel) and untreated (lower panel) MC38 (C) and B16.OVA (D) tumors. (E–F) The percentage of survival for MC38 (E) or B16.OVA (F) tumor-bearing mice is shown over time. The numbers under each graph represent the fraction of mice which achieved complete tumor regression. Data represent two independent experiments of a total of three (MC38 model) or two (B16.OVA model) experiments with five to six mice per group. Two-way analyses of variance (ANOVAs) (C–D) or log-rank (E–F) tests were used to assess significance. Significant differences are displayed for comparisons of each single-treatment group with the BO-112 + DMXAA group (** $p < 0.01$, *** $p < 0.001$, **** $p < 0.0001$). DMXAA, 5,6-dimethylxanthenone-4-acetic acid.

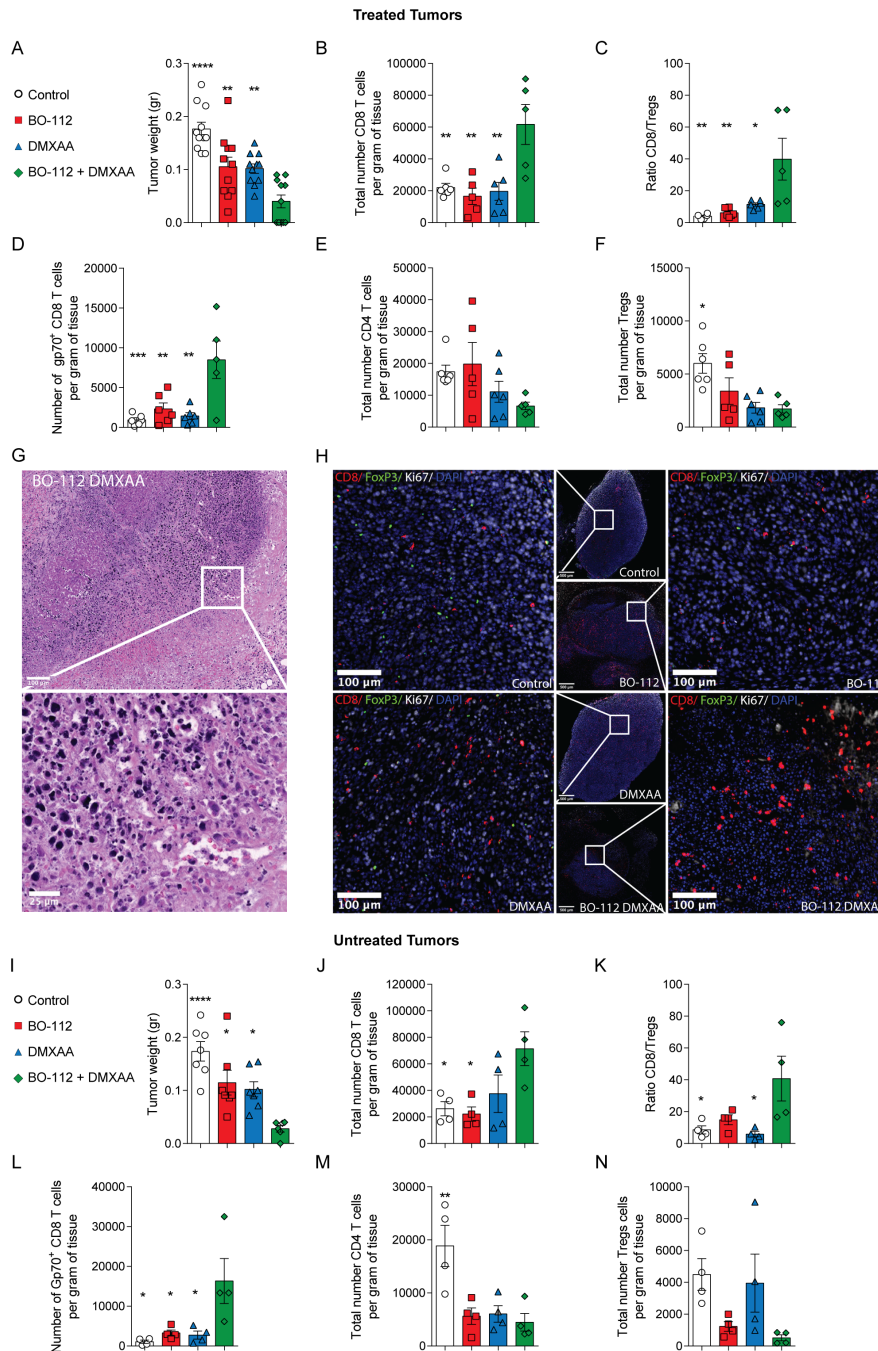


Figure 3 The intratumoral treatment with BO-112 and the STING agonist DMXAA increases the presence of effector CD8 T cells in the tumor microenvironment in both directly treated and untreated tumors. MC38 tumor-bearing mice received two doses of BO-112 and/or DMXAA following the dose regimen described in figure 1A and tumors and tumor draining lymph nodes (dLN) were collected 24 hours after the last treatment. Experimental group results are color coded as indicated. (A) The weight of tumors is shown for each treatment on day +11. (B) Total number of CD8 T cells per gram of tissue. (C) The ratio between CD8 and Tregs in the tumors is shown. (D) The number of gp70⁺ CD8 T cells is shown per gram of tumor. (E–F) Number of CD4 (D) and CD4 Tregs (E) per gram of tissue. (G) Representative microphotograph of H&E-stained sections from inflamed tissue that surrounds the area where intratumoral BO-112/DMXAA-treated tumors had been located and rejected, with magnification of the indicated region of interest. Scale bars represent 100 μm and 25 μm. (H) Representative images of multiplexed immunofluorescence of treated tumors stained for CD8, FOXP3, Ki67 and diaminido-2-phenylindole with magnifications of the indicated regions of interest. Scale bars represent 500 μm and 100 μm. (I–N) In separate experiments in which untreated contralateral tumors were excised 72 hours following the two-treatment schedule, tumor weight (I), density of CD8 T cells (J), ratio CD8/Tregs (K), content of gp70 antigen-specific CD8 T cells (L), CD4 T cell density (M) and Treg density (N) were assessed. Data represent an experiment with six or five mice per group for flow cytometry or tissue immunofluorescence analyses, respectively (mean ± SEM). A one-way analysis of variance (ANOVA) was used to assess significance. Significant differences are displayed for comparisons of each single-treatment group with the BO-112 + DMXAA group (*p < 0.05, **p < 0.01, ***p < 0.001, ****p < 0.0001). DMXAA, 5,6-dimethylxanthenone-4-acetic acid.

T cells specific for the gp70 immunodominant tumor epitope with H2-k^b pentamers, a synergistic increase in their numbers per gram of tumor tissue was observed (figure 3D). In contrast, the numbers of conventional CD4 T cells (CD4+Foxp3⁻) within the tumor microenvironment were not altered by intratumoral co-injections of BO-112 and the STING agonist (figure 3E), while Tregs (CD4+CD25+Foxp3⁺) followed a trend towards a reduction in their numbers (figure 3F). To confirm these findings, we evaluated the CD8 T cell and Treg component of treated tumors by multiplexed tissue immunofluorescence. Strikingly, four out of five cases of co-treated malignant tissues were completely necrotic and surrounded by an infiltrate in which neutrophils were prominent (figure 3G). Both DMXAA and BO-112 increased CD8 T cells and reduced Foxp3⁺ lymphocytes and this was also noticeable in the only case of co-treated tumors in which a DAPI/Ki67⁺ tumor region remained observable (figure 3H).

Regarding the tumor dLNs, even if size and cell content were markedly increased by intratumoral treatments (online supplemental figure 3A), we were not able to detect synergistic numeric increases of CD8 T cell lymphocytes or Gp70-specific CD8 T cells as a result of co-treatment, at least at the time point of analysis (online supplemental figure 3B–D). Each intratumoral treatment agent increased content of CD8 T cells and tumor-specific CD8 T cells in the spleen, but no changes could be attributed to the combination of intratumoral agents (online supplemental figure 3A–D).

From the point of view of circulating cytokines, BO-112 resulted in a clear increase in type I IFNs, IL-12, IL-18, TNF α and CXCL10 chemokine (online supplemental figure 2). However, STING agonist either did not cause systemic circulating elevations or only enhanced those observed on treatment with BO-112. These patterns may become important to avoid safety concerns due to overt systemic inflammation or cytokine release syndromes.

Important lymphocyte presence changes were observed in contralateral tumors 72 hours following treatment regimen completion, with such untreated tumors already decreasing size (figure 3I). These changes on combined injection included increases in CD8 T cell density (figure 3J), increases CD8/Treg ratios (figure 3K) and, importantly, increases in density of CD8 T lymphocytes recognizing the Gp70 tumor antigen (figure 3L). Both BO-112 and DMXAA as well as the combination reduced the density of CD4 T cells and BO-112 or the combination reduced Tregs (figure 3M and N). Similar observations were made in the B16.OVA tumor model (online supplemental figure 4A–F). Notably, in this B16.OVA model, increases in the density of CD8 T lymphocytes recognizing ovalbumin were observed in the microenvironment of the untreated distant tumor lesions (online supplemental figure 4D).

The absolute requirements for CD8 T cells were confirmed in selective depletion experiments that demonstrated CD8 T cell dependency, whereas CD4⁺ and NK1.1⁺ lymphocytes were dispensable (figure 4A–B). Of note, CD4 depletion improved efficacy in terms of survival (figure 4B), as previously reported for single agent BO-112. This is most likely attributable to the depletion of Tregs.^{17 36}

The efficacy on non-injected contralateral tumors following co-injection of BO-112 plus DMXAA is probably explained by CD8 T cells reaching the untreated tumor sites. Indeed, results in figure 3L and online supplemental figure 4D indicated more abundance of tumor-specific CTLs in the untreated tumor site on combined treatment in both the MC38 and B16.OVA tumor models. To assess if T cell recirculation was required for efficacy, experiments were performed on blockade of sphingosine 1-phosphate receptor with FTY720. As shown in online supplemental figure 5, FTY720 treatment completely abolished contralateral efficacy, while ipsilateral efficacy was preserved.

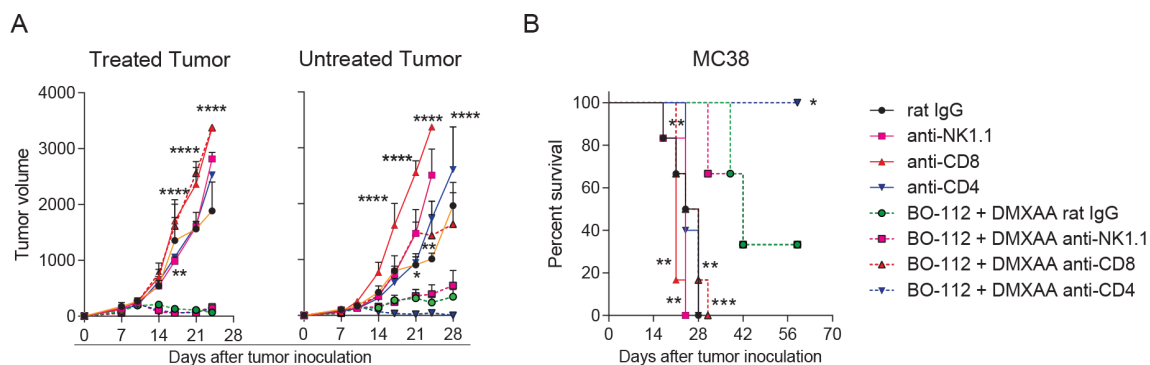


Figure 4 CD8 T cells are critical for the synergistic effects of BO-112 and DMXAA intratumoral co-injections. MC38 tumor-bearing mice were treated as described in figure 1A. Mice received intraperitoneal injections of rat IgG, anti-NK1.1, anti-CD8 β or anti-CD4 to deplete NK/NKT, CD8 and/or CD4 T cells respectively as color coded in the graphs. (A) The mean (\pm SEM) of tumor size (mm³) is shown for treated (left panel) and untreated (right panel) tumors. (B) The percentage of surviving mice is shown over time. Data are representative of two independent experiments with six mice per group (mean \pm SEM). Two-way analyses of variance (ANOVAs) (A) or log-rank (B) test were used to assess significance. Significant differences are displayed for comparisons of each group with BO-112 +DMXAA group without depletion (* p <0.05, ** p <0.01, *** p <0.001, **** p <0.0001). DMXAA, 5,6-dimethylxanthenone-4-acetic acid.

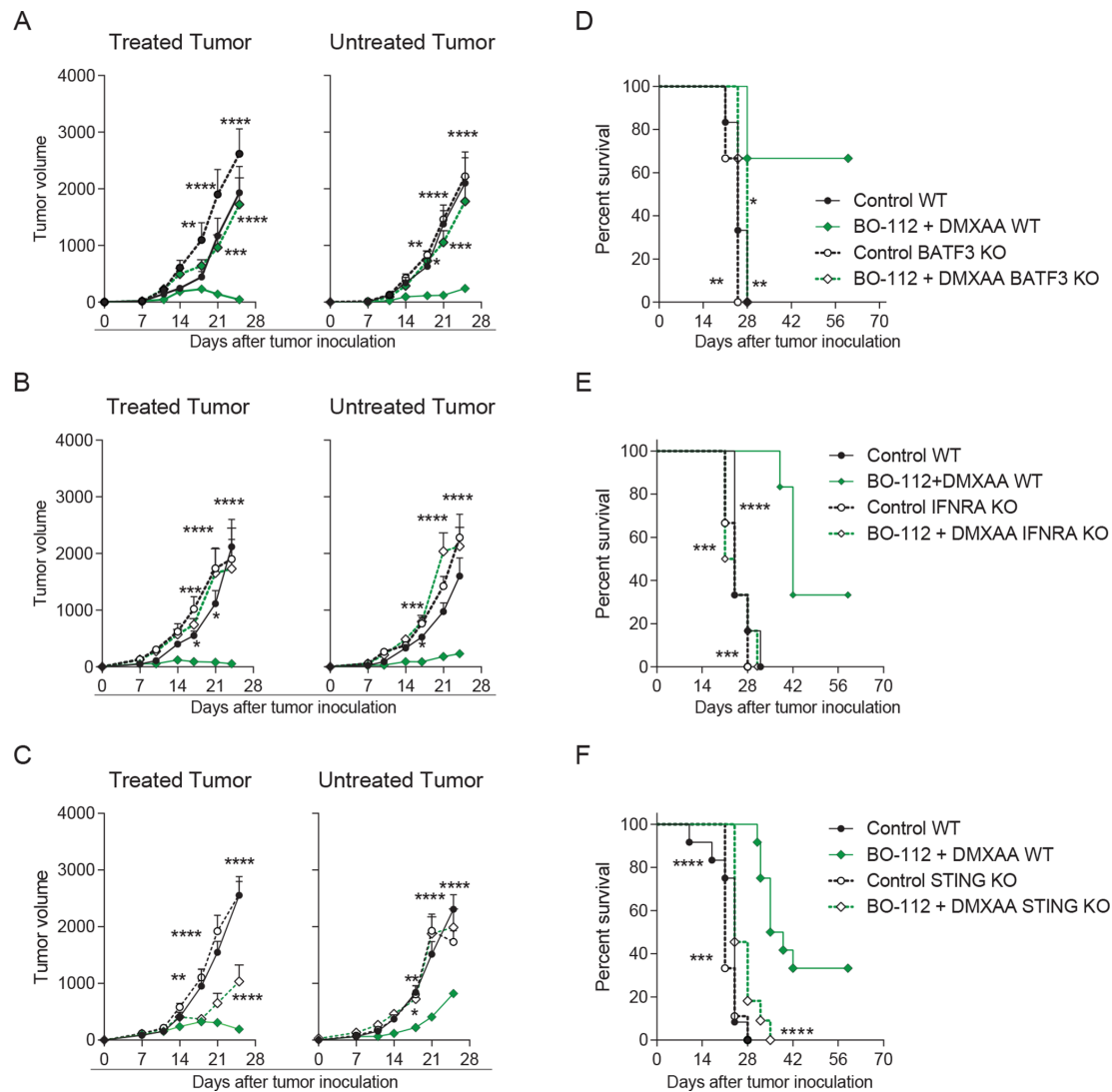


Figure 5 Conventional type 1 dendritic cells (cDC1), endogenous expression of type I interferon receptors and STING function in the host mouse are critical for the combined local and distant effects (A–C) The average of in vivo tumor growth (mm^3) is shown for treated (left panel) and untreated (right panel) tumors in BATF3 (A), IFNAR (B) or STING (C) knockout mice. (B) The percentage of survival is shown for BATF3 (D), interferon- α/β receptor (IFNAR) (E) or STING (F) knockout mice. Data are representative of two independent experiments with five to six mice per group (mean \pm SEM). Two-way analyses of variance (ANOVAs) (A–C) or log-rank (D–F) tests were used to assess significance. Significant differences are displayed for comparisons of each single-treatment group with the BO-112 +DMXAA group (* $p < 0.05$, ** $p < 0.01$, *** $p < 0.001$, **** $p < 0.0001$). BATF3, basic leucine zipper ATF-like transcription factor 3; DMXAA, 5,6-dimethylxanthenone-4-acetic acid.

All considered, bilateral efficacy on intratumoral co-injection of BO-112 and DMXAA requires the function of CTLs, which at some point must recirculate from the treated site to the non-treated lesions.

cDC1, STING and responsiveness to type I IFN in the host mouse are required for combined antitumor efficacy

Given the known mechanism of action of BO-112 and STING agonists and the key role of CD8 T cells for their efficacy,^{17 21 22} we examined the requirements for CD8 T cell cross-priming in the antitumor effects of the intratumoral co-injections. As shown in figure 5A, BATF3-dependent cDC1, which are essential for CD8 T cell cross-priming, were crucial for the local and contralateral efficacy of BO-112 and DMXAA following intratumoral

co-injections. Furthermore, both agents are known to induce type I IFN responses^{17 37 38} that are also critical for the CD8 T cell cross-priming by cDC1 cells.^{39 40} According to this notion, we found that the local and contralateral beneficial effects of intratumoral co-injections of BO-112 and DMXAA were lost in mice unresponsive to type I IFN due to the lack of IFNAR1, even if the tumor cells kept their IFN receptors intact (figure 5B). Lastly, we evaluated if the presence of STING was critical in the cells of tumor-bearing mice in order to generate synergy between BO-112 and DMXAA. Such seemed to be the case, since experiments in STING knockout mice showed a slight delay in tumor growth on the locally treated tumors, but no efficacy on the contralateral lesions when compared

with their WT counterparts (figure 5C). Consequently, the improvement on tumor-free survival caused by intratumoral co-injections with BO-112 and DMXAA was completely lost in tumor-bearing mice lacking BATF3, IFNAR1 or STING (figure 5D–F).

Regarding STING involvement, it could be possible that not only STING in the tumor-bearing host, but also in the tumor cells could be important for efficacy. To address this point, we used TSA breast cancer cells in which STING had been CRISPR/Cas9-silenced (online supplemental figure 6A) and were engrafted in BALB/c mice. Intratumoral treatment with BO-112 plus DMXAA exerted the ipsilateral and contralateral antitumor effects similarly to what was observed when using parental or mock-silenced control variants (online supplemental figure 6B, C). These results are interpreted in the sense that STING expression by malignant cells is dispensable for the synergistic bilateral antitumor effects.

The necessary involvement of cDC1 in the antitumor synergistic effects of BO-112 and DMXAA co-treatment prompted experiments on the cDC1-like mouse cell line MutuDC1.²⁸ Exposure of such dendritic cells to BO-112, DMXAA or the combination of both agents resulted in a very high production of cytokines and chemokines (online supplemental figure 7A). Interestingly, the combination of BO-112 and DMXAA gave rise to markedly increased outputs of IFN α , IL-2, CCL3 and TNF α over single-agent stimulated cultures (online supplemental figure 7A). In terms of maturation-denoting markers, both agents readily increased the surface expression of MHCII, CD86 and PD-L1, but BO-112 resulted in higher CD80 upregulation without any observable additive effects from both compounds in this regard, except for PD-L1 expression (online supplemental figure 7B). Moreover, similar experiments were performed on cDC1 cultures generated by culturing bone marrow cell suspensions with GM-CSF and FLT3L.²⁹ As shown in online supplemental figure 7A, D, prominent increases of type I IFNs were recapitulated as well as increases in TNF α and maturation makers, with a prominent increase of CD40 surface expression (online supplemental figure 7D). Maturation/activation of cDC1 could be entertained as one of the mechanisms underlying the synergistic efficacy of BO-112 and DMXAA with a postulated prominent role for upregulation of type I IFNs.

In addition to upregulation of cDC1 functions, changes in their numbers and density could be important as well. In this regard, both MC38 (online supplemental figure 8) and B16.OVA tumors (online supplemental figure 9) showed a tendency to increase contents of cDC1 in the tumor microenvironment of excised tumors. Of interest, such increases were also observed in the contralateral untreated tumors and more prominently so in the case of B16.OVA tumors (online supplemental figure 8 and 9). Treatment-associated changes in cDC2 content were not detected (online supplemental figure 8B and 9B). We also analyzed the content of CD11b+Ly6C+ myeloid cells, which did not change in the MC38 treated and untreated

tumors, at least at the analyzed time points (online supplemental figure 8C).

The prominent role for type I IFN and type I IFN-induced genes was also highlighted by RNAseq studies on co-treated or single-agent treated tumors 24 hours following single intratumoral injections, although no qualitative or quantitative differences in transcripts were found to explain the synergistic effects (online supplemental figure 10A–B).

Collectively, experiments on BATF3 KO, functional effects on cultured cDC1 cells and changes in their intratumoral contents support the role of cDC1 cells in the observed synergistic efficacy. Importantly, the strong type I IFN induction observed is likely to underlie synergistic efficacy, as also indicated by the experiments in IFNAR KO mice.

Preserved efficacy even if the co-injection of BO-112 and DMXAA was performed in separate tumors

To ascertain if co-injections were required or could be spatially separated in different lesions, experiments were set up in mice bearing three tumor nodules as outlined in figure 6A. Local and distant efficacy was reproduced on co-injections of BO-112 and DMXAA in the same tumor lesion leading to activity against the two distant untreated tumors with marked tumor growth delays when compared with control groups (figure 6B–C). Interestingly, when two different lesions were separately treated with BO-112 or DMXAA, efficacy against both treated tumors was preserved and in eight out of 12 mice third-party untreated tumor lesions also completely regressed (figure 6B–C). These findings lead to the conclusion that both treatments could be exerting their antitumor effect from separate injected tumor metastases, while preserving systemic efficacy.

In a simpler experimental setting, mice bearing two MC38-derived tumors were also co-treated in the same lesion with the two agents or treated with each agent in a separate tumor (online supplemental figure 11A). In this experiment, applying the agents to separate tumor lesions exerted comparable therapeutic efficacy as that observed on co-injection in terms of tumor size and survival (online supplemental figure 11B and C).

Intratumoral co-injections of BO-112 and the DMXAA STING agonist attain greater efficacy if combined with PD-1 blockade

PD-1 blockade is frequently used as a backbone in immunotherapy combinations including intratumoral immunotherapy.^{41–42} Hence, we tested in B16.OVA bilateral tumors if the efficacy of co-injections with BO-112 and the DMXAA STING agonist, which is suboptimal in this tumor model, could be increased. Systemic PD-1 blockade via intraperitoneal anti-PD-1 mAb injections along with intratumoral BO-112 and DMXAA co-administrations enhanced the efficacy against non-directly injected tumors (figure 7A–B). As a result, half of the mice receiving this

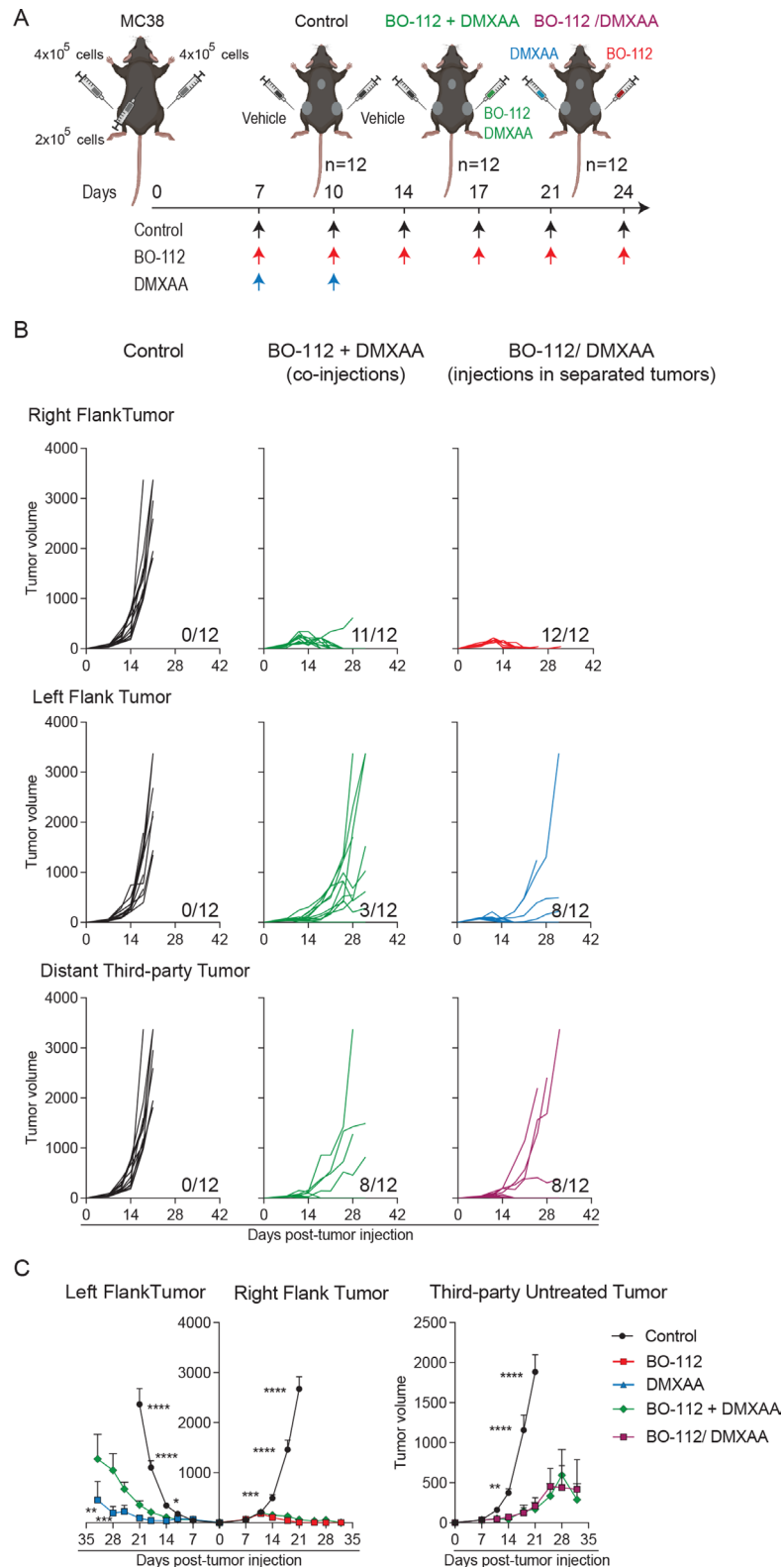


Figure 6 Co-injections in the same tumor lesion are not required for local and distant synergistic efficacy as assessed in mice bearing three tumor lesions. (A) Schematic representation of the dose regimen followed. (B) Graphical representation of the tumor volume (mm^3) over time for each individual mouse. Upper panels represent the in vivo tumor growth for the right flank treated tumors, middle panels represent the in vivo tumor growth for the left flank treated tumors and the lower panel represents in vivo tumor growth for distant untreated third-party tumors. The numbers under each graph represent the fraction of mice that achieved complete tumor regression. (C) The average tumor growth ($\text{mean} \pm \text{SEM}$) is shown. Data are representative of two independent experiments with six mice per group ($\text{mean} \pm \text{SEM}$). A two-way analysis of variance (ANOVA) was used to assess significance. Significant differences are displayed for comparisons of each single-treatment group with the BO-112 + DMXAA group (* $p < 0.05$, ** $p < 0.01$, *** $p < 0.001$, **** $p < 0.0001$). DMXAA, 5,6-dimethylxanthenone-4-acetic acid.

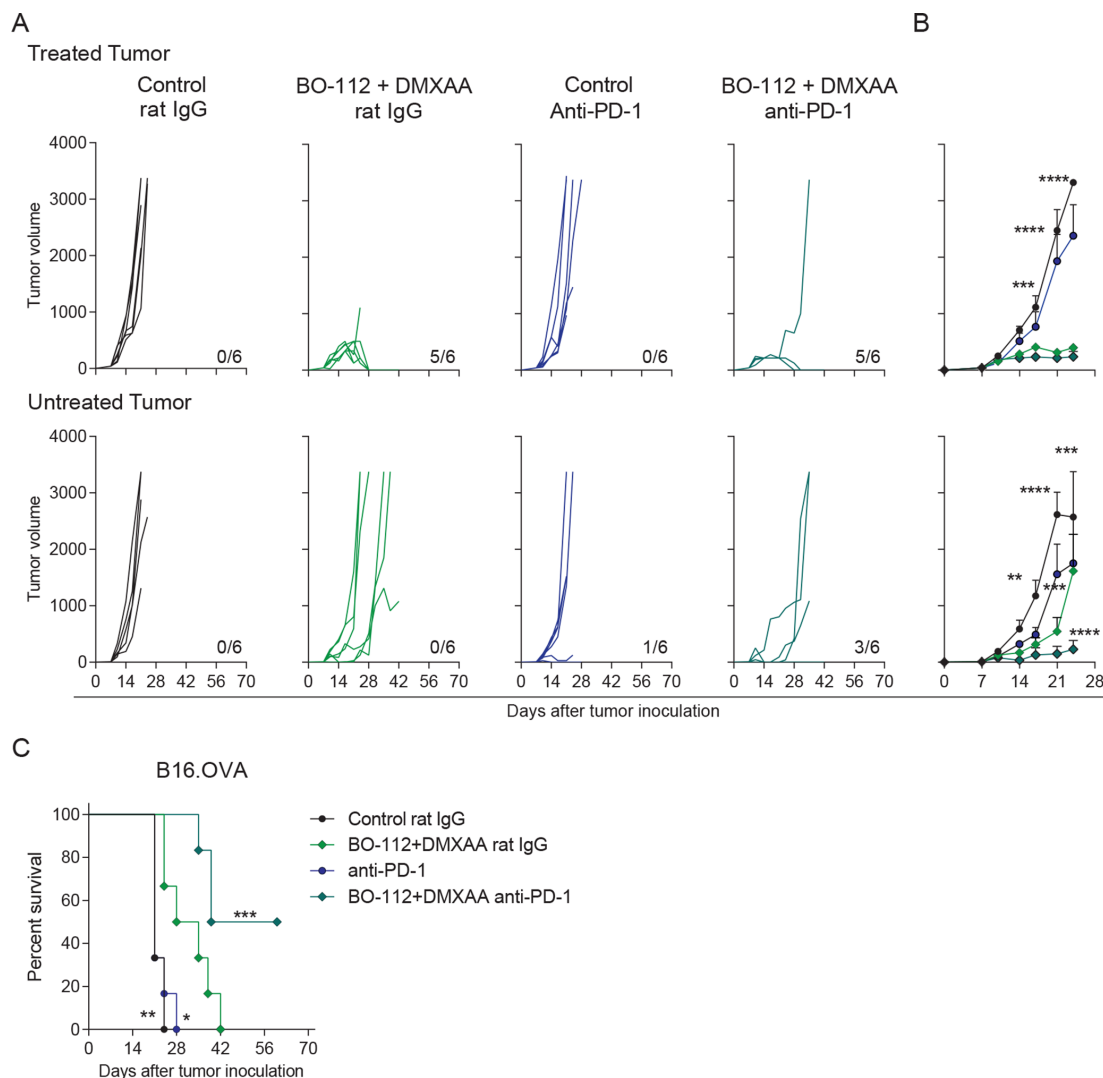


Figure 7 Combination of systemic PD-1 blockade and intratumoral co-injection of BO-112 +DMXAA increases abscopal efficacy. B16.OVA tumor bearing mice were treated as described in figure 1A. Mice received anti-PD-1 mAb or control rat IgG on days 8, 10 and 12 post-tumor cell inoculation. (A) Individual tumor growth (mm^3) is shown for each treatment group showing injected (upper panels) and untreated (lower panels) tumors. The numbers under each graph represent the fraction of mice which achieved complete tumor regression. (B) The average tumor size (mean \pm SEM) is followed for treated (upper panel) and untreated (lower panel) tumors. (C) The percentage of survival is shown over time. Data represent an experiment with six mice per group (mean \pm SEM). Two-way analyses of variance (ANOVAs) (B) or log-rank (C) tests were used to assess statistical significance. Statistically significant differences are displayed for comparisons of each group with the rat IgG +BO-112+DMXAA group (* p <0.05, ** p <0.01, *** p <0.001, **** p <0.0001). DMXAA, 5,6-dimethylxanthenone-4-acetic acid; mAb, monoclonal antibody; PD-1, programmed cell death protein 1.

therapeutic strategy rejected both tumors, resulting in a clear increase of overall survival (figure 7C).

DISCUSSION

Intratumoral immunotherapy has been thus far mainly developed with single agents. These schemes involve intratumoral or locoregional delivery of an agent that is sometimes vehicled with substances that facilitate pharmacokinetics and pharmacodynamics or protect and extend the action of the immunologically active compound.^{2 43} However, given that immunotherapy agents could act cooperatively, intratumoral co-injections of several agents with potential for synergy makes a great

deal of sense. The concept was pioneered by Ronald Levi's group on lymphoma-bearing mice treated intratumorally with cytotoxic T-lymphocyte-associated protein 4 (CTLA-4), anti-tumor necrosis factor receptor superfamily member 4 (TNFRSF4 or OX40) and CpG oligonucleotide co-injections.⁴⁴ This group also used local low-dose radiotherapy to further augment the in situ vaccination effects.⁴⁵

Inspired by those notions, we have explored the intratumoral combination of BO-112 and STING agonists since both of these compounds are actively undergoing clinical trials.^{12 23 24} First, intratumoral co-injection of such agents seems to be safe with regard to the well-being of the

mice at least in terms of behavior and nutritional status. Second, co-formulations should be feasible in the clinic for administration with already existing human STING agonists.^{37 38}

Co-injection was extremely efficacious against locally injected MC38 tumors and attained efficacy against contralateral tumors that were refractory to either single-agent therapy, thereby establishing the proof of concept for synergistic effects. In our hands, such a potent synergy could not be found with the other combinations of BO-112 tested with additional intratumoral agents, although other combinations, including viral vectors,⁴⁶ remain to be explored. Furthermore, our data do not exclude the possibility of CpG ODN-based agents in these combinations, although we selected STING agonist because of more evident synergy even if CpG Class C monotherapy also exerted effects on the contralateral tumors. In our opinion, co-injections of STING agonists plus dsRNA-based agents are not going to be the only intratumoral immunotherapy agents able to synergize on co-injection.

The described mechanisms of action for BO-112 and STING agonists^{17 38} are known to partially overlap, but still offered an opportunity to influence different pathways and cell types.^{5 47} Indeed, we might be seeing in tumor tissues the mimicry of intracellular viral or bacterial infection⁴⁸ that is perceived by the detection of dsRNA and gene stress or the ectopic cytoplasmic presence of DNA. For instance, during RNA viral infection, virus RNA should coexist with nuclear and mitochondrial DNA coming from dying or dead infected cells. Both elements denote danger and infection in such a manner that might have evolutionary converge to ensure that an immune response only takes place on dangerous infections.⁴⁹ Interestingly, some level of local tumor cell death is described to take place following BO-112 single-agent intratumoral delivery.^{12 17}

Our experiments reveal that very strong tumor-specific CD8 T cell-mediated immune responses are behind the synergy. Such a response is contingent on cDC1-mediated cross-priming,⁵⁰ which is postulated to be synergistically enhanced by BO-112 plus DMXAA co-treatment and seems to reflect this activity on cultured cDC1-like cells. Experiments on cultured MutuDC1 cells²⁸ and cDC1 BM-derived cultures²⁹ showed a very prominent increase in the secretion of type I IFNs on combined stimulation with BO-112 and DMXAA. The necessary role of cDC1 uncovered by BATF3-deficient mice and the need for IFNAR in the tumor bearing host, together with the increased type I IFN secretion, collectively suggest a train of events conducive to more robust antitumor CTL responses. We have not observed quantitative differences in macrophages infiltrating tumors at the analyzed time points, but functional changes remain to be explored in accordance to previous reports.^{51 52}

Certainly, more powerful CTLs may explain the systemic therapeutic effects, as CD8 T cell and cross-priming dependency has been previously described for both agents when applied as single-agent intratumoral treatments.^{17 21 22}

Contralateral effects on uninjected tumors are associated with more abundance of tumor antigen-specific CD8 T cells and cDC1 cells in these distant locations. The exact train of events sensitizing the contralateral non-injected tumors for the immunotherapy intervention remain to be seen. However, we have observed that FTY720-inhibitable T cell re-circulation is required for contralateral, but not for ipsilateral efficacy.

BO-112 via TLR3 and MDA5 would converge with STING activation towards the TBK1-IFN α/β signaling axis.^{17 18 53} We surmise that this signaling route is also induced at the level of engrafted malignant cells, but our results in knockout mouse strains indicate that the effects required for therapeutic efficacy take place mainly in endogenous cells of the tumor bearing mice. Once induced, the type I IFN system exerts multiple antitumor effects that chiefly induce local enhancement of antigen presentation/cross-presentation^{39 54} and critical effects on responding cDC1 and CD8 T cells.^{39 55–57} It is of note, that chronic STING and type I IFN activation in tumor cells could be deleterious,⁵⁸ perhaps suggesting that intermittent exposure to these intratumorally applied stimuli is preferable. Our transcriptomic data also support the key involvement of type I IFNs, although no evident transcriptional differences at 24 hours following single dose intratumoral injections were found to explain the synergy.

To our surprise, BO-112 and STING agonists could be delivered to separate tumor lesions while still preserving synergistic effects against third-party untreated tumor lesions. Thus, our results indicate that the mechanisms can be spatially separated while preserving most of the efficacy, which could offer some advantages in terms of the clinical translation of this therapeutic approach. In fact, we have not optimized the doses and schedules of the BO-112 + DMXAA combination. With STING agonist, relatively low doses are preferred since raising doses has been shown to reduce the intensity of CD8 T cell responses.²² With regard to local TLR3 agonists, there is no available evidence for deleterious effects from overdosing⁵⁹ and this provides an opportunity for dose and schedule refinements. For the time being, we have conducted our experiments based on the previously reported single-agent doses.^{17 22}

Our study opens up the pathway to other intratumoral immunotherapy combinations that might include a means for gene transfer using immunity enhancing transgenes, including virotherapy.^{4 46} Addition of systemic PD-1 blockade to the treatment regimen is frequently contemplated in development and we have found at least additive effects with intratumoral co-injection of BO-112 plus a STING agonist. The postulated train of events is that type I IFN, and eventually IFN γ from tumor-reactive T cells, induces PD-L1 expression on malignant cells. Therefore, blocking this negative feedback loop makes mechanistic sense as we had previously reported with RNA viral vectors encoding IL-12.⁶⁰ In our view, using pathogen-associated molecular patterns (PAMPs) instead of viral vectors for combined intratumoral immunotherapy may be more

convenient because of feasibility of simpler pharmaceutical combinations. For instance, combining additional intratumoral agents together with talimogene laherparepvec to increase efficacy seems more difficult in our opinion if compared with PAMPs.

The need in the clinic for combined approaches such as the one proposed here is obvious, since neither agent has shown sufficient antitumor efficacy when intratumorally administered as monotherapy. All things considered, BO-112 and STING agonists can be separately formulated, injected into human-accessible tumor metastases and nothing precludes co-injections using the same route or even the same syringe.⁶¹ With a view to the clinic, dose and schedule optimizations of each agent will be necessary, but in our opinion, co-formulation in a single preparation is a definite alternative. Further opportunities may involve irradiation of locally injected lesions (Rodríguez-Ruiz ME *et al.*, manuscript in preparation). In any case, the objective is to achieve not only local control of the injected disease but more importantly, efficacy against distant tumor lesions, as our experiments in mice bearing bilateral tumors have revealed.

Author affiliations

¹Immunology and Immunotherapy, Center for Applied Medical Research (CIMA), University of Navarra, Pamplona, Spain

²Navarra Institute for Health Research (IdiSNA), Pamplona, Spain

³Centro de Investigación Biomedica en Red de Cáncer (CIBERONC), Madrid, Spain

⁴Pathology, Clínica Universidad de Navarra, Pamplona, Spain

⁵Immunology and Oncology, Clínica Universidad de Navarra, Pamplona, Spain

⁶Radiation Oncology, Weill Cornell Medicine, New York, New York, USA

⁷Oncology, Highlight Therapeutics, Valencia, Spain

Acknowledgements The authors thank Dr. Kenneth M. Murphy, Dr. Matthew Albert, Dr. Gloria Gonzalez Aseguinolaza, Dr. Lieping Chen, Dr. Karl E. Hellström and Dr. Hans AchaOrbea for their kind contribution to this project with mouse strains and cell lines. The authors also thank Dr. Beatriz Tavira for her support with the Luminex™ MAGPIX™ instrument system. The authors also thank both CIMA shared flow cytometry and animal facilities for their technical support. The authors thank Dr. Paul Miller for professional English editing. Finally, the authors thank all the members of Dr. Melero's group for the valuable help and discussion throughout the course of this project.

Contributors MA designed and performed research, analyzed data, and wrote the manuscript. CM and MF contributed conducting experiments. CEDA and MV performed the H&E and the immunofluorescence assays. JGG conducted the RNAseq bioinformatics analysis. XF and WHS provided STING KO cell lines. CEDA, MF, MV, MCO, AT, JGV, FA, MFS, PB, MQ provided scientific input and assisted with the preparation of the manuscript. IM had experimental oversight, wrote the manuscript and is the guarantor of this manuscript. All authors have read and agreed to the published version of the manuscript.

Funding This work has been supported by MINECO SAF2017-83267-C2-1-R (AEI/FEDER, UE). This project has received funding from the European Union's Horizon 2020 research and innovation program (grant agreement n° 635122 - PROCROP), the Spanish Association Against Cancer's Investigator (AECC), the Ministerio de Ciencia e Innovación and the Agencia Estatal de Investigación (RTC2019-006860-1), the Instituto de Salud Carlos III (PI19/01128, and PI20/00002) co-financed by Fondos Feder, Gobierno de Navarra Proyecto LINTERNA (Ref.: 0011-1411-2020-000075) and the Instituto de Salud Carlos III (PI20/00002) co-financed by Fondos FEDER "A way to make Europe". MA is supported by the AECC's Investigator grant (INVEST19041ALVA). MF is supported by a fellowship of the Aid Program Assigned to Projects from the University of Navarra. AT has received financial support through "la Caixa" Banking Foundation (LCF/BQ/LR18/11640014). FA receives a Miguel Servet I (CP19/00114) contract from ISCIII (Instituto de Salud Carlos III) co-financed by FSE (Fondo Social Europeo) "Investing in your future". MFS is supported by a Miguel Servet contract MS17/00196 and a grant project

PI19/00668 from Instituto de Salud Carlos III, Fondo de Investigación Sanitaria (Spain).

Competing interests MA, CM, CEDA, MF, MV, JGG, MCO, JGV, AT, FA, MER, FX, WHS and PB declare no competing interests. MFS reports receiving research funding from Roche. MQ is full-time employee of Highlight Therapeutics. IM reports receiving commercial research grants from BMS, Highlight Therapeutics, Alligator, Pfizer Genmab and Roche; has received speakers bureau honoraria from MSD; and is a consultant or advisory board member for BMS, Roche, AstraZeneca, Genmab, Pharmamar, F-Star, Bioncotech, Bayer, Numab, Pieris, Gossamer, Alligator and Merck Serono.

Patient consent for publication Not applicable.

Ethics approval All animal protocols were approved by the Ethics Committee of Animal Experimentation at University of Navarra.

Provenance and peer review Not commissioned; externally peer reviewed.

Data availability statement All data relevant to the study are included in the article or uploaded as supplementary information. Data and materials are available upon reasonable request.

Supplemental material This content has been supplied by the author(s). It has not been vetted by BMJ Publishing Group Limited (BMJ) and may not have been peer-reviewed. Any opinions or recommendations discussed are solely those of the author(s) and are not endorsed by BMJ. BMJ disclaims all liability and responsibility arising from any reliance placed on the content. Where the content includes any translated material, BMJ does not warrant the accuracy and reliability of the translations (including but not limited to local regulations, clinical guidelines, terminology, drug names and drug dosages), and is not responsible for any error and/or omissions arising from translation and adaptation or otherwise.

Open access This is an open access article distributed in accordance with the Creative Commons Attribution Non Commercial (CC BY-NC 4.0) license, which permits others to distribute, remix, adapt, build upon this work non-commercially, and license their derivative works on different terms, provided the original work is properly cited, appropriate credit is given, any changes made indicated, and the use is non-commercial. See <http://creativecommons.org/licenses/by-nc/4.0/>.

ORCID iDs

Maite Alvarez <http://orcid.org/0000-0002-5969-9181>

Pedro Berraondo <http://orcid.org/0000-0001-7410-1865>

Ignacio Melero <http://orcid.org/0000-0002-1360-348X>

REFERENCES

- Marabelle A, Kohrt H, Caux C, *et al.* Intratumoral immunization: a new paradigm for cancer therapy. *Clin Cancer Res* 2014;20:1747–56. doi:10.1158/1078-0432.CCR-13-2116
- Aznar MA, Tinari N, Rullán AJ, *et al.* Intratumoral delivery of immunotherapy-act locally, think globally. *J Immunol* 2017;198:31–9. doi:10.4049/jimmunol.1601145
- Marabelle A, Tselikas L, de Baere T, *et al.* Intratumoral immunotherapy: using the tumor as the remedy. *Ann Oncol* 2017;28:xii33–43. doi:10.1093/annonc/mdx683
- Harrington K, Freeman DJ, Kelly B, *et al.* Optimizing oncolytic virotherapy in cancer treatment. *Nat Rev Drug Discov* 2019;18:689–706. doi:10.1038/s41573-019-0029-0
- Vanpouille-Box C, Hoffmann JA, Galluzzi L. Pharmacological modulation of nucleic acid sensors - therapeutic potential and persisting obstacles. *Nat Rev Drug Discov* 2019;18:845–67. doi:10.1038/s41573-019-0043-2
- Fransen MF, van der Sluis TC, Ossendorp F, *et al.* Controlled local delivery of CTLA-4 blocking antibody induces CD8+ T-cell-dependent tumor eradication and decreases risk of toxic side effects. *Clin Cancer Res* 2013;19:5381–9. doi:10.1158/1078-0432.CCR-12-0781
- Hewitt SL, Bai A, Bailey D, *et al.* Durable anticancer immunity from intratumoral administration of IL-23, IL-36γ, and OX40L mRNAs. *Sci Transl Med* 2019;11. doi:10.1126/scitranslmed.aat9143. [Epub ahead of print: 30 01 2019].
- Etcheberria I, Bolaños E, Quetglas JI, *et al.* Intratumor adoptive transfer of IL-12 mRNA transiently engineered antitumor CD8+ T cells. *Cancer Cell* 2019;36:613–29. doi:10.1016/j.ccell.2019.10.006
- Ressler JM, Karasek M, Koch L, *et al.* Real-Life use of talimogene laherparepvec (T-VEC) in melanoma patients in centers in Austria, Switzerland and Germany. *J Immunother Cancer* 2021;9:e001701. doi:10.1136/jitc-2020-001701

- 10 Frank MJ, Reagan PM, Bartlett NL, et al. *In Situ* Vaccination with a TLR9 agonist and local low-dose radiation induces systemic responses in untreated indolent lymphoma. *Cancer Discov* 2018;8:1258–69. doi:10.1158/2159-8290.CD-18-0743
- 11 Ribas A, Medina T, Kummar S, et al. SD-101 in combination with pembrolizumab in advanced melanoma: results of a phase Ib, multicenter study. *Cancer Discov* 2018;8:1250–7. doi:10.1158/2159-8290.CD-18-0280
- 12 Márquez-Rodas I, Longo F, Rodríguez-Ruiz ME, et al. Intratumoral nanoplexed poly I:C BO-112 in combination with systemic anti-PD-1 for patients with anti-PD-1-refractory tumors. *Sci Transl Med* 2020;12. doi:10.1126/scitranslmed.abb0391. [Epub ahead of print: 14 10 2020].
- 13 Kyi C, Roudko V, Sabado R, et al. Therapeutic immune modulation against solid cancers with intratumoral Poly-I:CLC: a pilot trial. *Clin Cancer Res* 2018;24:4937–48. doi:10.1158/1078-0432.CCR-17-1866
- 14 Hewitt SL, Bailey D, Zielinski J, et al. Intratumoral IL12 mRNA therapy promotes Th1 transformation of the tumor microenvironment. *Clin Cancer Res* 2020;26:6284–98. doi:10.1158/1078-0432.CCR-20-0472
- 15 Algazi AP, Twitty CG, Tsai KK, et al. Phase II trial of IL-12 plasmid transfection and PD-1 blockade in immunologically quiescent melanoma. *Clin Cancer Res* 2020;26:2827–37. doi:10.1158/1078-0432.CCR-19-2217
- 16 Tselikas L, Champiat S, Sheth RA, et al. Interventional radiology for local immunotherapy in oncology. *Clin Cancer Res* 2021;27:2698–705. doi:10.1158/1078-0432.CCR-19-4073
- 17 Aznar MA, Planelles L, Perez-Olivares M, et al. Immunotherapeutic effects of intratumoral nanoplexed poly I:C. *J Immunother Cancer* 2019;7:116. doi:10.1186/s40425-019-0568-2
- 18 Tormo D, Chечиńska A, Alonso-Curbelo D, et al. Targeted activation of innate immunity for therapeutic induction of autophagy and apoptosis in melanoma cells. *Cancer Cell* 2009;16:103–14. doi:10.1016/j.ccr.2009.07.004
- 19 Kalbasi A, Tariveranmohabadi M, Hakimi K, et al. Uncoupling interferon signaling and antigen presentation to overcome immunotherapy resistance due to JAK1 loss in melanoma. *Sci Transl Med* 2020;12. doi:10.1126/scitranslmed.abb0152. [Epub ahead of print: 14 10 2020].
- 20 Corrales L, Gajewski TF. Molecular pathways: targeting the stimulator of interferon genes (STING) in the immunotherapy of cancer. *Clin Cancer Res* 2015;21:4774–9. doi:10.1158/1078-0432.CCR-15-1362
- 21 Corrales L, Glickman LH, McWhirter SM, et al. Direct activation of sting in the tumor microenvironment leads to potent and systemic tumor regression and immunity. *Cell Rep* 2015;11:1018–30. doi:10.1016/j.celrep.2015.04.031
- 22 Sivick KE, Desbrien AL, Glickman LH, et al. Magnitude of therapeutic sting activation determines CD8⁺ T cell-mediated anti-tumor immunity. *Cell Rep* 2018;25:3074–85. doi:10.1016/j.celrep.2018.11.047
- 23 Harrington KJ, Brody J, Ingham M, et al. Preliminary results of the first-in-human (FIH) study of MK-1454, an agonist of stimulator of interferon genes (STING), as monotherapy or in combination with pembrolizumab (pembro) in patients with advanced solid tumors or lymphomas. *Annals of Oncology* 2018;29:viii712–12.
- 24 Zandberg DP, Ferris R, Laux D, et al. 71P a phase II study of ADU-S100 in combination with pembrolizumab in adult patients with PD-L1+ recurrent or metastatic HNSCC: preliminary safety, efficacy and PK/PD results. *Annals of Oncology* 2020;31:S1446–7. doi:10.1016/j.annonc.2020.10.559
- 25 Hildner K, Edelson BT, Purtha WE, et al. Batf3 deficiency reveals a critical role for CD8alpha+ dendritic cells in cytotoxic T cell immunity. *Science* 2008;322:1097–100. doi:10.1126/science.1164206
- 26 Schilte C, Couderc T, Chretien F, et al. Type I IFN controls Chikungunya virus via its action on nonhematopoietic cells. *J Exp Med* 2010;207:429–42. doi:10.1084/jem.20090851
- 27 Sauer J-D, Sotelo-Troha K, von Moltke J, et al. The N-Ethyl-N-Nitrosourea-Induced *Goldenticket* Mouse Mutant Reveals an Essential Function of *Sting* in the *In Vivo* Interferon Response to *Listeria monocytogenes* and Cyclic Dinucleotides. *Infect Immun* 2011;79:688–94. doi:10.1128/IAI.00999-10
- 28 Fuertes Marraco SA, Grosjean F, Duval A, et al. Novel murine dendritic cell lines: a powerful auxiliary tool for dendritic cell research. *Front Immunol* 2012;3:331. doi:10.3389/fimmu.2012.00331
- 29 Minute L, Teijeira A, Sanchez-Paulete AR, et al. Cellular cytotoxicity is a form of immunogenic cell death. *J Immunother Cancer* 2020;8:e000325. doi:10.1136/jitc-2019-000325
- 30 Alvarez M, Simonetta F, Baker J, et al. Indirect impact of PD-1/PD-L1 blockade on a murine model of NK cell exhaustion. *Front Immunol* 2020;11:7. doi:10.3389/fimmu.2020.00007
- 31 Alvarez M, Simonetta F, Baker J, et al. Regulation of murine NK cell exhaustion through the activation of the DNA damage repair pathway. *JCI Insight* 2019;4. doi:10.1172/jci.insight.127729
- 32 Abengozar-Muela M, Esparza MV, Garcia-Ros D, et al. Diverse immune environments in human lung tuberculosis granulomas assessed by quantitative multiplexed immunofluorescence. *Mod Pathol* 2020;33:2507–19. doi:10.1038/s41379-020-0600-6
- 33 Bolger AM, Lohse M, Usadel B. Trimmomatic: a flexible trimmer for Illumina sequence data. *Bioinformatics* 2014;30:2114–20. doi:10.1093/bioinformatics/btu170
- 34 Dobin A, Davis CA, Schlesinger F, et al. Star: ultrafast universal RNA-seq aligner. *Bioinformatics* 2013;29:15–21. doi:10.1093/bioinformatics/bts635
- 35 Ritchie ME, Phipson B, Wu D, et al. limma powers differential expression analyses for RNA-sequencing and microarray studies. *Nucleic Acids Res* 2015;43:e47. doi:10.1093/nar/gkv007
- 36 Sánchez-Paulete AR, Teijeira Alvaro, Quetglas JI, et al. Intratumoral immunotherapy with XCL1 and sFlt3L encoded in recombinant Semliki Forest virus-derived vectors fosters dendritic cell-mediated T-cell Cross-Priming. *Cancer Res* 2018;78:6643–54. doi:10.1158/0008-5472.CAN-18-0933
- 37 Gajewski TF, Higgs EF. Immunotherapy with a sting. *Science* 2020;369:921–2. doi:10.1126/science.abc6622
- 38 Flood BA, Higgs EF, Li S, et al. Sting pathway agonism as a cancer therapeutic. *Immunol Rev* 2019;290:24–38. doi:10.1111/imr.12765
- 39 Le Bon A, Etchart N, Rossmann C, et al. Cross-priming of CD8+ T cells stimulated by virus-induced type I interferon. *Nat Immunol* 2003;4:1009–15. doi:10.1038/ni978
- 40 Woo S-R, Fuertes MB, Corrales L, et al. Sting-dependent cytosolic DNA sensing mediates innate immune recognition of immunogenic tumors. *Immunity* 2014;41:830–42. doi:10.1016/j.immuni.2014.10.017
- 41 Ribas A, Wolchok JD. Cancer immunotherapy using checkpoint blockade. *Science* 2018;359:1350–5. doi:10.1126/science.aar4060
- 42 Sharma P, Siddiqui BA, Anandhan S, et al. The next decade of immune checkpoint therapy. *Cancer Discov* 2021;11:838–57. doi:10.1158/2159-8290.CD-20-1680
- 43 Fransen MF, Cordfunke RA, Sluijter M, et al. Effectiveness of slow-release systems in CD40 agonistic antibody immunotherapy of cancer. *Vaccine* 2014;32:1654–60. doi:10.1016/j.vaccine.2014.01.056
- 44 Houot R, Levy R. T-Cell modulation combined with intratumoral CpG cures lymphoma in a mouse model without the need for chemotherapy. *Blood* 2009;113:3546–52. doi:10.1182/blood-2008-07-170274
- 45 Brody JD, Ai WZ, Czerwinski DK, et al. In situ vaccination with a TLR9 agonist induces systemic lymphoma regression: a phase I/II study. *J Clin Oncol* 2010;28:4324–32. doi:10.1200/JCO.2010.28.9793
- 46 Macedo N, Miller DM, Haq R, et al. Clinical landscape of oncolytic virus research in 2020. *J Immunother Cancer* 2020;8:e001486. doi:10.1136/jitc-2020-001486
- 47 Gajewski TF, Schreiber H, Fu Y-X. Innate and adaptive immune cells in the tumor microenvironment. *Nat Immunol* 2013;14:1014–22. doi:10.1038/ni.2703
- 48 Jensen J, Chen ZJ. Bacteria sting viral invaders. *Nature* 2020;586:363–4. doi:10.1038/d41586-020-02712-8
- 49 Iwasaki A, Medzhitov R. Control of adaptive immunity by the innate immune system. *Nat Immunol* 2015;16:343–53. doi:10.1038/ni.3123
- 50 Wculek SK, Cueto FJ, Mujal AM, et al. Dendritic cells in cancer immunology and immunotherapy. *Nat Rev Immunol* 2020;20:7–24. doi:10.1038/s41577-019-0210-z
- 51 Ohkuri T, Kosaka A, Ishibashi K, et al. Intratumoral administration of cGAMP transiently accumulates potent macrophages for anti-tumor immunity at a mouse tumor site. *Cancer Immunology, Immunotherapy* 2017;66:705–16. doi:10.1007/s00262-017-1975-1
- 52 Muraoka D, Seo N, Hayashi T, et al. Antigen delivery targeted to tumor-associated macrophages overcomes tumor immune resistance. *Journal of Clinical Investigation* 2019;129:1278–94. doi:10.1172/JCI97642
- 53 Chen M, Hu S, Li Y, et al. Targeting nuclear acid-mediated immunity in cancer immune checkpoint inhibitor therapies. *Signal Transduct Target Ther* 2020;5:270. doi:10.1038/s41392-020-00347-9
- 54 Hervas-Stubbs S, Perez-Gracia JL, Rouzaut A, et al. Direct effects of type I interferons on cells of the immune system. *Clin Cancer Res* 2011;17:2619–27. doi:10.1158/1078-0432.CCR-10-1114
- 55 Hervas-Stubbs S, Mancheño U, Riezu-Boj J-I, et al. Cd8 T cell priming in the presence of IFN- α renders CTLs with improved responsiveness to homeostatic cytokines and recall antigens: important traits for adoptive T cell therapy. *Ji*. 2012;189:3299–310. doi:10.4049/jimmunol.1102495



- 56 Kolumam GA, Thomas S, Thompson LJ, *et al.* Type I interferons act directly on CD8 T cells to allow clonal expansion and memory formation in response to viral infection. *J Exp Med* 2005;202:637–50. doi:10.1084/jem.20050821
- 57 Gajewski TF, Corrales L. New perspectives on type I IFNs in cancer. *Cytokine Growth Factor Rev* 2015;26:175–8. doi:10.1016/j.cytogfr.2015.01.001
- 58 Ablasser A, Chen ZJ. cGAS in action: expanding roles in immunity and inflammation. *Science* 2019;363. doi:10.1126/science.aat8657. [Epub ahead of print: 08 03 2019].
- 59 Le Naour J, Galluzzi L, Zitvogel L, *et al.* Trial Watch: TLR3 agonists in cancer therapy. *Oncoimmunology* 2020;9:1771143. doi:10.1080/2162402X.2020.1771143
- 60 Quetglas JI, Labiano S, Aznar M Ángela, *et al.* Virotherapy with a semliki forest virus-based vector encoding IL12 synergizes with PD-1/PD-L1 blockade. *Cancer Immunol Res* 2015;3:449–54. doi:10.1158/2326-6066.CIR-14-0216
- 61 Melero I, Castanon E, Alvarez M, *et al.* Intratumoural administration and tumour tissue targeting of cancer immunotherapies. *Nat Rev Clin Oncol* 2021;18:558–76.